Gold Bull (2015) 48:161–167
DOI 10.1007/s13404-015-0174-0

ORIGINAL PAPER

Active metal (cadmium) doping enhanced the stability of inert metal (gold) nanocluster under O_2 atmosphere and the catalysis activity of benzyl alcohol oxidation

Huijuan Deng[1] · Shuxin Wang[1] · Shan Jin[1] · Sha Yang[1] · Yajie Xu[1] · Lingli Liu[1] · Ji Xiang[1] · Daqiao Hu[1] · Manzhou Zhu[1]

Published online: 11 December 2015

Abstract Compared with the inert metal (gold), the active metal (Cd) is much more prone to oxidation, leading to its high oxidation state. In this work, we found that doping the homogold $Au_{25}(SR)_{18}$ nanocluster with cadmium largely enhances its stability. The differential pulse voltammetry (DPV) analysis suggested that Cd doping raised the high occupied molecular orbital (HOMO) energy of homogold Au_{25} nanocluster, which led to stronger retention of its valence electrons. $Cd_1Au_{24}(SR)_{18}$ nanocluster also exhibited much higher activity than homogold Au_{25} nanocluster in aerobic benzyl alcohol oxidation.

Keywords Metal cluster · Doping · Synergistic effect · Aerobic oxidation catalysis · Oxidation · Differential pulse voltammetry

Introduction

Gold nanoclusters (NCs) with a few tens of metal atoms have emerged as a new class of nanomaterials with wide application [1–5]. By doping these small homogold nanoclusters with even single atom, many new physical and chemical properties are expressed [6–10]. In the past few years, significant advances have been made in the synthesis and property studies of these doping nanoclusters [6–21]. Among homogold nanoclusters, $Au_{25}(SR)_{18}$ nanocluster has been well studied due to its stable structure among three different charges (−1/0/+1) [22–26], which led to the exploration of a wide range of catalytic pathways facilitated by Au_{25} for organic reactions, such as oxidation [27–29], hydrogenation [30–32], electronic transfer reactions [26, 33], and electrocatalysis [34, 35]. Recent research implies that doping foreign atoms into this 25 noble metal system can largely affect the stability and the catalytic activity compared to the homogold counterpart [7–10, 17–19]. Compared with these inert metal doped $(M\text{-}Au)_{25}$ (M=Pt/Pd/Cu/Ag) nanoclusters, the research on highly active metal (such as Cd) being used to dope into the nanocluster was rarely studied. This gives rise to an interesting question, "What metal synergistic effects are at work between the noble (low activity) metal and the high activity metal in the atomically precise nanoclusters?"

Herein, we use the well-determined high-activity metal doped $Cd_1Au_{24}(SR)_{18}{}^0$ and homogold $Au_{25}(SR)_{18}$ nanocluster (Scheme 1) as a model to study how the active-metal dopant affects the optical, stabilization, and catalysis properties of the homogold nanoclusters. It is found that the active metal (Cd) doping led the nanocluster to be much more stable than the $Au_{25}(SR)_{18}$ nanocluster under an oxidizing environment and harder to lose its free valence electron to produce the seven free valence electronic $Cd_1Au_{24}(SR)_{18}{}^+$ nanocluster. This new finding is opposite to the common sense (high-activity metal is less stable than noble metal; for example, gold is much more stable than Fe). Furthermore, after removal of the ligands, this doped nanocluster shows much more catalytic activity in benzyl alcohol oxidation reaction.

✉ Daqiao Hu
hudaqiao@ahu.edu.cn

✉ Manzhou Zhu
zmz@ahu.edu.cn

[1] Department of Chemistry and Center for Atomic Engineering of Advanced Materials, Anhui University, Hefei, Anhui 230601, People's Republic of China

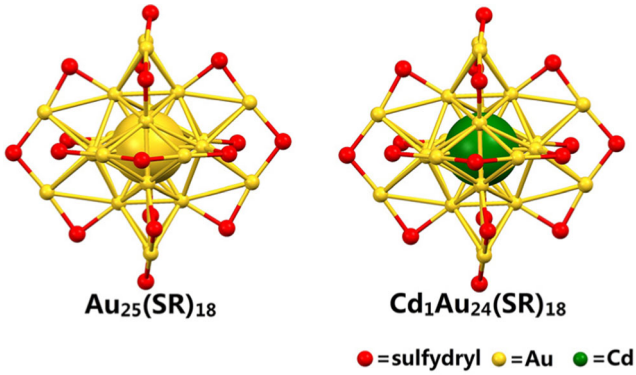

Scheme 1 Crystal structure of activity metal (Cd) doping $Cd_1Au_{24}(SR)_{18}$ [10] and homogold $Au_{25}(SR)_{18}$ [24] nanocluster. Color label: *red*, sulfhydryl; *yellow*, gold; *green*, Cd

Experimental section

Chemicals and instruments

All reagents and solvents were commercially purchased and used as received without further purification, including tetrachloroauric(III) acid ($HAuCl_4\ 3H_2O$, ≥99.99 % metal basis), $CdCl_2$ (99 %), tetraoctylammonium bromide (TOAB, ≥98 %), 2-Phenylethanethiol ($PhCH_2CH_2SH$, ≥99.99 %), sodium borohydride (≥98 %), toluene (HPLC, ≥99.9 %), methylene chloride (HPLC, ≥99.9 %), methanol (HPLC, ≥99.9 %), and trans-2-[3-(4-tert-butylphenyl)-2-methyl-2-propenylidene]malononitrile (DCTB, ≥98 %). All glassware was cleaned with aqua regia (HCl/HNO_3=3:1 vol %), rinsed with copious nanopure water, and then dried in an oven prior to use. Matrix-assisted laser desorption ionization mass spectrometry (MALDI-MS) was performed on an Applied Bruker Autoflex MALDI-TOF equipped with a nitrogen laser (337 nm). The mass spectra were collected in the linear mode at an acceleration voltage of 25 kV and a delay time of 350 ns. trans-2-[3-(4-tert-Butyl-phenyl)-2-methyl-2-propenylidene]malononitrile (DCTB) was used as the matrix.

Optical spectroscopic studies were carried out with an Agilent 8453 diode array spectrometer, and solution samples were prepared using toluene as the solvent.

The oxidation of aerobic benzyl alcohol was studied using gas chromatography (Shimadzu, GC-2010, Japan). The obtained solution was purified, diluted to 100 mL, and analyzed by gas chromatography (Shimadzu, GC-2010, Japan). Quantitative analysis was performed using the external standard method. Transmission electron microscopy (TEM) images were collected by JEM 2100 of JEOL (Japan).

Preparation of $Au_{25}(SC_2H_4Ph)_{18}$ nanoclusters

The monodisperse $[Au_{25}(SR)_{18}]^-TOA^+$ nanoclusters were prepared following the reported method [24]. Typically, 10 mL of a toluene solution of TOAB (0.252 g) was added to 5 mL of an aqueous solution of $HAuCl_4\ 3H_2O$ (800 μL, 0.4 mmol). The solution was vigorously stirred with a magnetic stir bar to facilitate phase transfer of the Au(III) salt into the toluene phase. After ~15 min, phase transfer was completed, leaving a clear aqueous layer at the bottom of the flask; the aqueous layer was then pipetted off. The toluene solution of TOAB-Au(III) precursor complex was then cooled down to 0 °C in an ice bath over a period of 30 min under magnetic stirring. $PhCH_2CH_2SH$ (0.18 mL) was added; the deep red solution turned to faint yellow over a period of ~5 min and finally to clear over ~1 h.

After the solution turned clear, the stirring speed was changed to fast stirring, and immediately, an aqueous solution of $NaBH_4$ (0.155 g, freshly made in 10 mL ice-cold nanopure water) was quickly added all at once. The reaction was allowed to proceed overnight. The mixture was washed several times with CH_3OH to remove the lingering ligand and by-products. Finally, pure $Au_{25}(SR)_{18}$ nanoclusters were obtained through extraction using acetonitrile. The as-prepared products showed three distinct absorption bands at 400, 450, and 670 nm, which are characteristic peaks of Au_{25} clusters.

Preparation of $Cd_1(SC_2H_4Ph)_2$

$CdCl_2$ metal salts (0.3 g) was dissolved in a mixture solution (5 mL; 1:4 water/ethanol). Another ethanol solution containing $PhCH_2CH_2SH$ (0.6 mL) and triethylamine (0.5 mL) was added to the first made mixture solution under vigorous stirring. After 30 min stir-mixing, the contents were taken to a centrifuge tube. The solution was then removed and the precipitate was washed several times with ethanol/water to remove the lingering $PhCH_2CH_2SH$ leading to the isolation of the pure solid $Cd_1(SC_2H_4Ph)_2$.

Preparation of $Cd_1Au_{24}(SC_2H_4Ph)_{18}$ nanoclusters

The $Cd_1Au_{24}(SR)_{18}$ nanoclusters with high molecular purity were prepared following a synthetic method reported recently [10]. Ten milligrams of $Au_{25}(SC_2H_4Ph)_{18}^-$ was dissolved in 10 mL toluene, and 10 mg $Cd_1(SC_2H_4Ph)_2$ (powder) was then added to the solution. The reaction was allowed to proceed for 2 h at room temperature. After that, the reaction mixture was transferred to a centrifuge tube and centrifuged at ~9000 rpm. The organic layer was separated from the precipitate and evaporated to dryness. The dried nanoclusters were washed with methanol at least three times and collected by centrifugation. The final product was then extracted from the precipitate using a mixed DCM/MeCN solution. $Cd_1Au_{24}(SR)_{18}$ was then recrystallized in a toluene–ethanol mixed solvent.

Typical procedure for the catalysis benzyl alcohol oxidation reaction

The aerobic oxidation of benzyl alcohol was performed under room temperature. Typically, benzyl alcohol (50 μL) and K_2CO_3 (28 mg) were mixed well in toluene (2 mL) in a test tube. The mixture was then transferred to the synthesizer under vigorous stirring at 25 °C. The Au_{25} and Cd_1Au_{24} catalysts (25 mg, 25 mg) were added into the solution before purging with tert-butyl hydroperoxide (TBHP), respectively. After 24 h, the mixture was stopped. The obtained solution was analyzed by gas chromatograph. The conversion of benzyl alcohol is defined as the percentage of the total amount of benzyl alcohol consumed in the oxidation reaction to the total amount of benzyl alcohol at the initial time. The selectivity of the reaction is denoted as the ratio of benzyl alcohol converted to the corresponding products.

Results and discussion

Characterization of $Cd_1Au_{24}(SC_2H_4Ph)_{18}$

The UV−vis spectrum of the $Cd_1Au_{24}(SC_2H_4Ph)_{18}$ nanoclusters (Fig. 1) shows absorption peaks at 400, 480, and 650 nm, which are similar to the case of $Au_{25}(SC_2H_4Ph)_{18}$ nanoclusters at 400, 450, and 680 nm. In comparison with $Au_{25}(SC_2H_4PH)_{18}$, a blueshift of about 30 nm was found in the Cd doping $Cd_1Au_{24}(SR)_{18}$ nanocluster. Typically, the 680 nm absorption peak of homogold $Au_{25}(SR)_{18}$ nanocluster is assigned to the transitions from the high occupied molecular orbital (HOMO) of the Au 6sp orbital to the lowest unoccupied molecular orbital (LUMO) of the Au 6sp orbital (*sp*→*sp*). This indicates that the exchange of the Au to the Cd atom will have a distinct effect on the HOMO–LUMO transition and band gap.

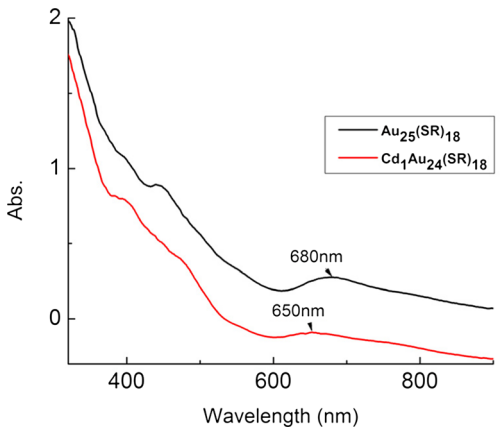

Fig. 1 Comparison of UV–vis spectra of *black line* $Au_{25}(SC_2H_4Ph)_{18}$ nanoclusters and *red line* $Cd_1Au_{24}(SC_2H_4Ph)_{18}$ nanoclusters

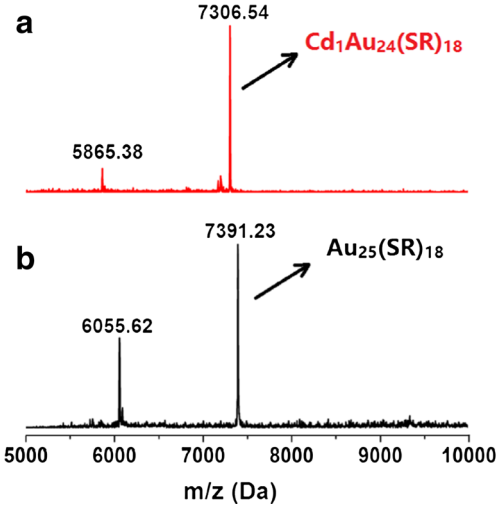

Fig. 2 MALDI-MS analysis of the two nanoclusters **a** $Cd_1Au_{24}(SC_2H_4Ph)_{18}$ and **b** $Au_{25}(SC_2H_4Ph)_{18}$

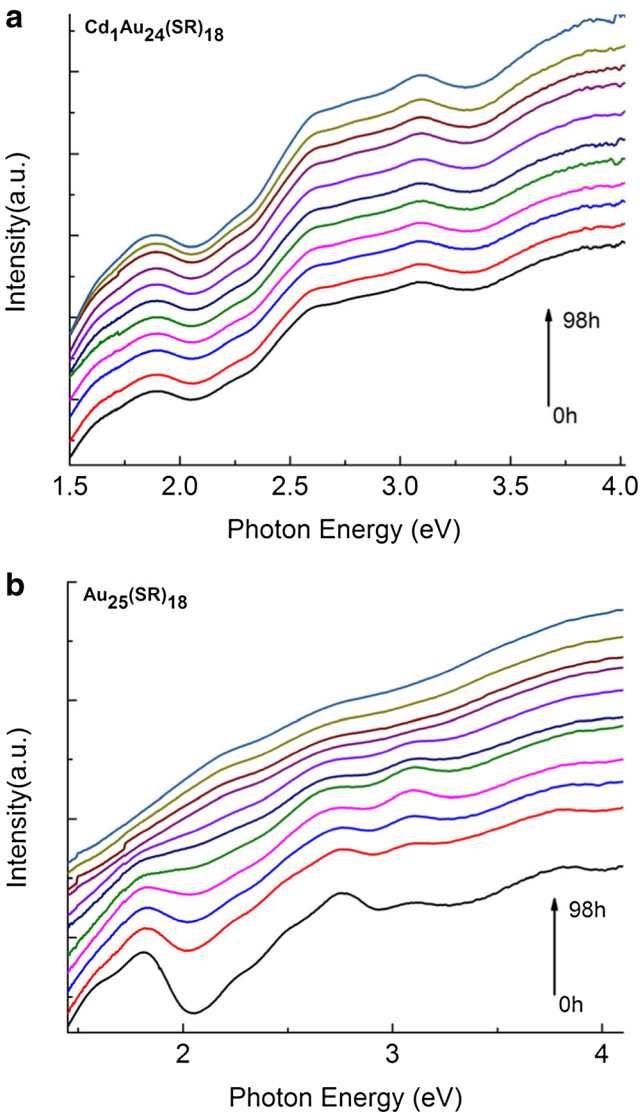

Fig. 3 Oxidation station track spectra of **a** $Cd_1Au_{24}(SR)_{18}$ and **b** $Au_{25}(SR)_{18}$ on the photon energy scales

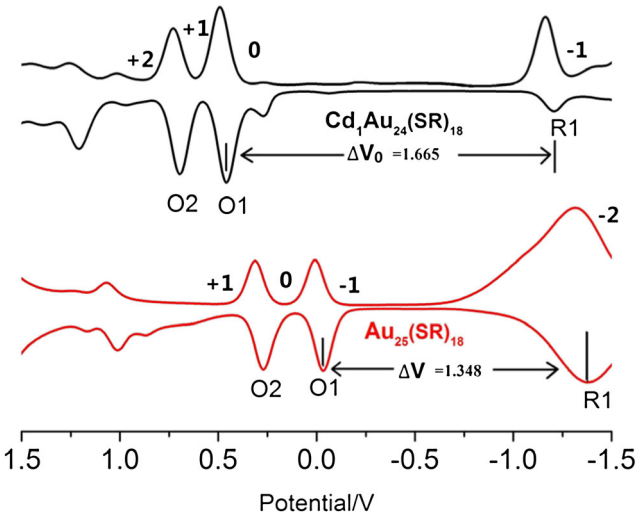

Fig. 4 Differential pulse voltammetry (DPV) of $Cd_1Au_{24}(SR)_{18}$ (*black line*) and $Au_{25}(SR)_{18}$ (*red line*) at 0.01 V/s in degassed CH_2Cl_2 containing 0.1 M Bu_4NPF_6 with 1 mm diameter Pt working, SCE reference, and carbon rod counter electrode

$Cd_1Au_{24}(SC_2H_4Ph)_{18}$ and $Au_{25}(SC_2H_4Ph)_{18}$ nanoclusters were further characterized by MALDI-TOF-MS. It should be pointed out that discriminating Cd (112.41 Da) from Au (196.97 Da) is not challenging because of their relatively huge mass difference (84.59 Da). In the MALDI-TOF-MS spectra, the peak at 7306.54 Da is assigned to the molecular ion peak of $Cd_1Au_{24}(SR)_{18}$ (Fig. 2a). Meanwhile, the peak at 7391.23 Da was assigned to the molecular ion peak of $Au_{25}(SR)_{18}$ (Fig. 2b). Other peaks were their fragment's peaks, upside (Fig. 2a) 5865.38 Da was assigned to $Au_{20}(SR)_{14}$ fragment peak of $Cd_1Au_{24}(SR)_{18}$, and 6055.62 Da (Fig. 2b) was assigned to $Au_{21}(SR)_{14}$ fragment peak of $Au_{25}(SR)_{18}$. All these results indicate that the precise formula of the cluster are $Cd_1Au_{24}(SC_2H_4Ph)_{18}$ and $Au_{25}(SR)_{18}$ nanoclusters, respectively. These results are consistent with the already reported X-ray crystallographic analysis.

Photon energy spectra were employed to investigate the stability of $Cd_1Au_{24}(SR)_{18}$ of resistance to oxygen atmospheres in comparison with its $Au_{25}(SR)_{18}$ counterpart. Both the pure $Cd_1Au_{24}(SR)_{18}$ and the $Au_{25}(SR)_{18}$ nanoclusters were dissolved in toluene then exposed to the pure O_2 atmosphere (one bar). As shown in Fig. 3b, the $Au_{25}(SR)_{18}^-$ nanocluster was first oxidized to neutral $Au_{25}(SR)_{18}^0$ [26] then the whole nanocluster decomposed slowly. The characteristic peaks of Au_{25} became flattened gradually and eventually disappeared, indicating that Au_{25} was completely decomposed. On the contrary, $Cd_1Au_{24}(SR)_{18}$ displayed stronger resistance to oxidation in the oxygen environment compared to $Au_{25}(SR)_{18}$. Figure 3a revealed that the spectrum of $Cd_1Au_{24}(SR)_{18}$ did not show obvious change in the pure O_2 after about 48 h and the final curve is identical to the first curve of $Cd_1Au_{24}(SR)_{18}$. Therefore, the Cd atom inserting in the Au core was instrumental in enhancing the resilience in oxygen atmospheres. In other words, the synergistic effect of the inter-metal promoted the stability of nanoclusters. Furthermore, these results demonstrate that Cd doping of the metal core of $Au_{25}(SR)_{18}$ is a powerful method for producing stable thiolate-protected M_{25} clusters with different electronic structures and physical properties from $Au_{25}(SR)_{18}$.

Typically, highly active metal is more unstable than noble metal in the metallic form; for example, cadmium could be easily oxidized to CdO under O_2 atmosphere, while gold cannot be. It is very interesting to find that active metal (Cd) doping enhanced the stability of gold nanocluster in the pure O_2 atmosphere. To achieve basic understanding of this abnormal phenomenon, differential pulse voltammetry (DPV) was used to find the difference in oxidation potential between $Cd_1Au_{24}(SR)_{18}$ and $Au_{25}(SR)_{18}$ nanoclusters.

As shown in Fig. 4, the current peaks for $Cd_1Au_{24}^{0/1+}$ and $Cd_1Au_{24}^{1+/2+}$ represent the successive removal of single electrons from the HOMO level. The peak for $Cd_1Au_{24}^{0/-1}$ represents the first reduction step (LUMO energy). Notably, the oxidation peaks shift to more positive (O1 = 0.456 V) potentials relative to $Au_{25}(SR)_{18}$ nanoclusters (O1 = −0.0333 V). At the same time, the electrochemical gap of Cd_1Au_{24} nanoclusters, ΔV_0, between the first oxidation peak and the first reduction peak (1.665 V), is larger than that of Au_{25} nanoclusters (1.348 V). These results clearly indicated that active metal (Cd) doping noble metal nanoclusters can largely raise the HOMO energy of homogold Au_{25} nanoclusters and finally lead to it being more difficult to be oxidized to its high valence state, which is opposite to the bulk metal.

Cd_1Au_{24} catalyzes the benzyl alcohol oxidation reaction in high efficiency

The benzyl alcohol oxidation reaction was initially used to evaluate the catalytic activity of the as-prepared Cd_1Au_{24}/CNT nanoclusters (Table 1) in contrast with homogold Au_{25}/CNT. The catalytic oxidation reaction was conducted at room temperature for 24 h. The obtained solution was analyzed with a gas chromatograph with a flame ionization detector by using an external standard method. Most notably, Au_{25}/CNT and Cd_1Au_{24}/CNT exhibited a visible difference in the catalysis: the conversion of the highly active metal doped (63 %) is nearly twice as high as the homogold catalyst (33 %). Also, we calculated the turnover number (TON) and turnover frequency (TOF) of both of these two nanoclusters, which suggested that Cd_1Au_{24} can largely enhance the catalytic activity of alcohol oxidation. On the basis of these results, we conclude that Cd atom doping is the main cause of the enhanced activities. Within the framework of this structural model, Au sites in Cd_1Au_{24}/CNT, which are more negative than those in Au_{25}/CNT due to electron transfer from Cd, may activate O_2 more effectively, and as a result,

Table 1 Reaction conditions: amount of catalyst, 25 mg; amount of $PhCH_2OH$, 50 μL; amount of K_2CO_3, 28 mg; volume of toluene, 2 mL; temperature, 25 °C; TBHP, 150 μL

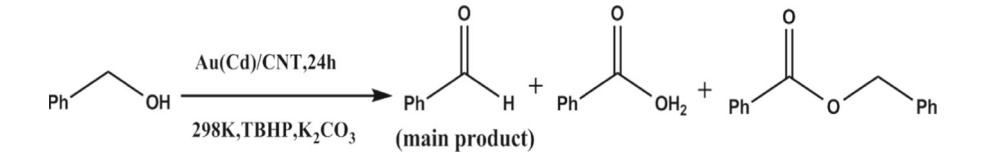

Entry	Catalyst	TON	TOF (/h)	Conversion (%)	Yield (%)	Benzaldehyde selectivity
1	Blank	0	0	0	0	0
2	CNT	0	0	0	0	0
3	$Au_{25}(SR)_{18}$	635.5	26.48	33 %	33 %	100 %
4	$Cd_1Au_{24}(SR)_{18}$	1162.9	48.45	62.8 %	60.7 %	96.7 %

Cd_1Au_{24}/CNT shows higher catalytic activity than Au_{25}/CNT for aerobic benzyl alcohol oxidation. As in our previous report [15], the accumulation of electronic charge density is found in the space between the Cd atom and the Au_{12} shell and the depletion of electronic charge density is at the Cd atom. Electronic charge density of Au sites has changed leading to electron transfer from Cd to Au. The central Cd atom is positively charged so that Au sites are more negative. This synergistic effect is proposed to be due to modulation of the electronic structures by intracluster electron transfer from Cd to Au.

TEM analysis of the catalysts before Fig. 5a, c and after Fig. 5b, d showed similar size distributions. These results demonstrate that the catalysts did not show obvious change before and after reactions.

Conclusions

In summary, this work reported that highly active metal (Cd) doping can largely enhance the stability of homogold Au_{25} nanocluster under the O_2 environment, which is opposed to

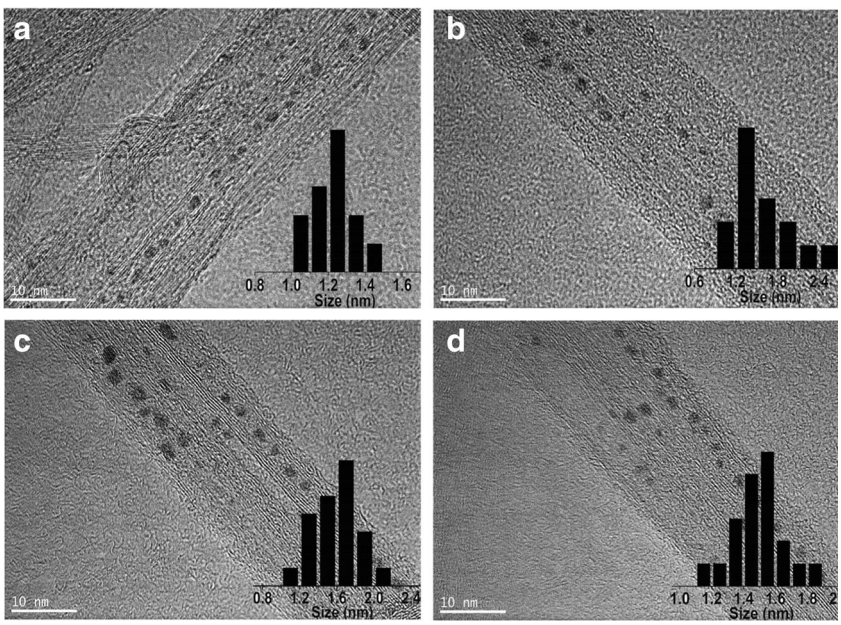

Fig. 5 Typical TEM images of Cd_1Au_{24}/CNT before (**a**) and after (**b**) catalysis. TEM images of Au_{25}/CNT before (**c**) and after (**d**) catalysis. Insets show the cluster size distributions before and after reactions

the bulk metal (cadmium is more easily oxidized than gold). The DPV revealed that Cd doping largely increased the HOMO–LUMO gap of homogold $Au_{25}(SR)_{18}$ nanocluster, through modulation of the HOMO level, which led this doped nanocluster to be much more stable in the O_2 environment. Lastly, active metal doping Cd_1Au_{24} nanocluster exhibits much higher catalytic activity than the homogold Au_{25} nanocluster in aerobic benzyl alcohol oxidation with higher yield and selectivity.

Acknowledgments This work was supported by the National Natural Science Foundation of China (21072001, 21372006), Ministry of Education, Anhui Province, and the 211 Project of Anhui University.

References

1. Jin R (2010) Quantum sized, thiolate-protected gold nanoclusters. Nanoscale 2(3):343–362. doi:10.1039/b9nr00160c
2. Jin R (2015) Atomically precise metal nanoclusters: stable sizes and optical properties. Nanoscale 7(5):1549–1565. doi:10.1039/c4nr05794e
3. Shang L, Dong S, Nienhaus GU (2011) Ultra-small fluorescent metal nanoclusters: synthesis and biological applications. Nano Today 6(4):401–418. doi:10.1016/j.nantod.2011.06.004
4. Li G, Jin R (2013) Atomically precise gold nanoclusters as new model catalysts. Acc Chem Res 46(8):1749–1758. doi:10.1021/ar300213z
5. Yamazoe S, Koyasu K, Tsukuda T (2014) Nonscalable oxidation catalysis of gold clusters. Acc Chem Res 47(3):816–824. doi:10.1021/ar400209a
6. Jin R, Nobusada K (2014) Doping and alloying in atomically precise gold nanoparticles. Nano Res 7(3):285–300. doi:10.1007/s12274-014-0403-5
7. Xie S, Tsunoyama H, Kurashige W, Negishi Y, Tsukuda T (2012) Enhancement in aerobic alcohol oxidation catalysis of Au_{25}Clusters by single Pd atom doping. ACS Catal 2(7):1519–1523. doi:10.1021/cs300252g
8. Negishi Y, Kurashige W, Niihori Y, Iwasa T, Nobusada K (2010) Isolation, structure, and stability of a dodecanethiolate-protected Pd_1Au_{24} cluster. Phys Chem Chem Phys 12(23):6219–6225. doi:10.1039/b927175a
9. Qian H, Jiang DE, Li G, Gayathri C, Das A, Gil RR, Jin R (2012) Monoplatinum doping of gold nanoclusters and catalytic application. J Am Chem Soc 134(39):16159–16162. doi:10.1021/ja307657a
10. Wang S, Song Y, Jin S, Liu X, Zhang J, Pei Y, Meng X, Chen M, Li P, Zhu M (2015) Metal exchange method using Au_{25} nanoclusters as templates for alloy nanoclusters with atomic precision. J Am Chem Soc 137(12):4018–4021. doi:10.1021/ja511635g
11. Yuan X, Dou X, Zheng K, Xie J (2015) Recent advances in the synthesis and applications of ultrasmall bimetallic nanoclusters. Part Part Syst Charact 32(6):613–629. doi:10.1002/ppsc.201400212
12. Bracey CL, Ellis PR, Hutchings GJ (2009) Application of copper-gold alloys in catalysis: current status and future perspectives. Chem Soc Rev 38(8):2231–2243. doi:10.1039/b817729p
13. Ferrando R, Jellinek J, Johnston RL (2008) Nanoalloys: from theory to applications of alloy clusters and nanoparticles. Chem Rev 108(3):845–910. doi:10.1021/cr040090g
14. Jia J, Wang Q (2009) Intensely luminescent gold(I)-silver(I) cluster with hypercoordinated carbon. J Am Chem Soc 131(46):16634–16635. doi:10.1021/ja906695h
15. Yang H, Wang Y, Lei J, Shi L, Wu X, Makinen V, Lin S, Tang Z, He J, Hakkinen H, Zheng L, Zheng N (2013) Ligand-stabilized $Au_{13}Cu_x$ (x = 2, 4, 8) bimetallic nanoclusters: ligand engineering to control the exposure of metal sites. J Am Chem Soc 135(26):9568–9571. doi:10.1021/ja402249s
16. Yang H, Wang Y, Yan J, Chen X, Zhang X, Hakkinen H, Zheng N (2014) Structural evolution of atomically precise thiolated bimetallic $[Au_{12+n}Cu_{32}(SR)_{30+n}]^{4-}$ (n = 0, 2, 4, 6) nanoclusters. J Am Chem Soc 136(20):7197–7200. doi:10.1021/ja501811j
17. Negishi Y, Iwai T, Ide M (2010) Continuous modulation of electronic structure of stable thiolate-protected Au_{25} cluster by Ag doping. Chem Commun 46(26):4713–4715. doi:10.1039/c0cc01021a
18. Negishi Y, Igarashi K, Munakata K, Ohgake W, Nobusada K (2012) Palladium doping of magic gold cluster $Au_{38}(SC_2H_4Ph)_{24}$: formation of $Pd_2Au_{36}(SC_2H_4Ph)_{24}$ with higher stability than $Au_{38}(SC_2H_4Ph)_{24}$. Chem Commun 48(5):660–662. doi:10.1039/c1cc15765e
19. Negishi Y, Munakata K, Ohgake W, Nobusada K (2012) Effect of copper doping on electronic structure, geometric structure, and stability of thiolate-protected Au nanoclusters. J Phys Chem Lett 3(16):2209–2214. doi:10.1021/jz300892w
20. Wang S, Meng X, Das A, Li T, Song Y, Cao T, Zhu X, Zhu M, Jin R (2014) A 200-fold quantum yield boost in the photoluminescence of silver-doped Ag_xAu_{25-x} nanoclusters: the 13th silver atom matters. Angew Chem Int Ed Engl 53(9):2376–2380. doi:10.1002/anie.201307480
21. Wang S, Jin S, Yang S, Chen S, Song Y, Zhang J, Zhu M (2015) Total structure determination of surface doping $[Ag_{46}Au_{24}(SR)_{32}](BPh_4)_2$ nanocluster and its structure-related catalytic property. Sci Adv 1:e1500441
22. Zhu M, Aikens CM, Hollander FJ, Schatz GC, Jin R (2008) Correlating the crystal structure of A thiol-protected Au_{25} cluster and optical properties. J Am Chem Soc 130(18):5883–5884. doi:10.1021/ja801173r
23. Heaven MW, Dass A, White PS, Holt KM, Murray RW (2008) Crystal structure of the gold nanoparticle $[N(C_8H_{17})_4][Au_{25}(SCH_2CH_2Ph)_{18}]$. J Am Chem Soc 130(12):3754–3755. doi:10.1021/ja800561b
24. Zhu M, Aikens CM, Hendrich MP, Gupta R, Qian H, Schatz GC, Jin R (2009) Reversible switching of magnetism in thiolate-protected Au_{25} superatoms. J Am Chem Soc 131(7):2490–2492. doi:10.1021/ja809157f
25. Antonello S, Perera NV, Ruzzi M, Gascon JA, Maran F (2013) Interplay of charge state, lability, and magnetism in the molecule-like $Au_{25}(SR)_{18}$ cluster. J Am Chem Soc 135(41):15585–15594. doi:10.1021/ja407887d
26. Liu Z, Zhu M, Meng X, Xu G, Jin R (2011) Electron transfer between $[Au_{25}(SC_2H_4Ph)_{18}]^-TOA^+$ and oxoammonium cations. J Phys Chem Lett 2(17):2104–2109. doi:10.1021/jz200925h
27. Nie X, Qian H, Ge QJ, Xu H, Jin R (2012) CO oxidation catalyzed by oxide-supported $Au_{25}(SR)_{18}$ nanoclusters and identification of perimeter sites as active centers. ACS Nano 6(7):6014–6022. doi:10.1021/nn301019f
28. Yoskamtorn T, Yamazoe S, Takahata R, Nishigaki J-i, Thivasasith A, Limtrakul J, Tsukuda T (2014) Thiolate-mediated selectivity control in aerobic alcohol oxidation by porous carbon-supported Au_{25}Clusters. ACS Catal 4(10):3696–3700. doi:10.1021/cs501010x

29. Liu Y, Tsunoyama H, Akita T, Tsukuda T (2010) Efficient and selective epoxidation of styrene with TBHP catalyzed by Au_{25} clusters on hydroxyapatite. Chem Commun 46(4):550–552. doi:10.1039/b921082b
30. Zhu Y, Qian H, Drake BA, Jin R (2010) Atomically precise Au25SR18 nanoparticles as catalysts for the selective hydrogenation of alpha, beta-unsaturated ketones and aldehydes. Angew Chem Int Ed Engl 49(7):1295–1298. doi:10.1002/anie.200906249
31. Yamamoto H, Yano H, Kouchi H, Obora Y, Arakawa R, Kawasaki H (2012) N, N-Dimethylformamide-stabilized gold nanoclusters as a catalyst for the reduction of 4-nitrophenol. Nanoscale 4(14): 4148–4154. doi:10.1039/c2nr30222e
32. Shivhare A, Ambrose SJ, Zhang H, Purves RW, Scott RW (2013) Stable and recyclable Au_{25} clusters for the reduction of 4-nitrophenol. Chem Commun 49(3):276–278. doi:10.1039/c2cc37205c
33. Chong H, Li P, Wang S, Fu F, Xiang J, Zhu M, Li Y (2013) Au_{25} clusters as electron-transfer catalysts induced the intramolecular cascade reaction of 2-nitrobenzonitrile. Sci Rep 10:3213–3214. doi:10.1038/srep03214
34. Kumar SS, Kwak K, Lee D (2011) Amperometric sensing based on glutathione protected Au_{25} nanoparticles and their pH dependent electrocatalytic activity. Electroanalysis 23(9):2116–2124. doi:10.1002/elan.201100240
35. Kauffman DR, Alfonso D, Matranga C, Qian H, Jin R (2012) Experimental and computational investigation of Au_{25} clusters and CO_2: a unique interaction and enhanced electrocatalytic activity. J Am Chem Soc 134(24):10237–10243. doi:10.1021/ja303259q